Electronic Supplementary Material (ESI) for Journal of Materials Chemistry A.
This journal is © The Royal Society of Chemistry 2018

Supporting Informations

Sulphur edge and vacancy assisted nitrogen-phosphorus co-doped exfoliated tungsten disulfide: a superior electrocatalyst in hydrogen evolution reaction

Anurupa Maiti[a] and Suneel Kumar Srivastava[a]*
Department of Chemistry
Indian Institute of Technology, Kharagpur-721302, India
E-mail: sunil111954@yahoo.co.uk.

S1

Room temperature XRD analysis is carried out on Philip Holland instrument using cu kα radiation (150.1 nm) at scan rate of 5^0/min in the range of 5-90^0. FT-IR analysis is carried out on Perkin Elmer instrument from 400-4000 cm^{-1} by KBR disc. The morphology of the samples were characterized by field emission scanning electron microscopy (FESEM) on Carl Zeiss operating at 20 kV respectively. TEM images were recorded on a TECNAI G2 SEI (Netherland) operating at 200 kV and Gatanmultipole charge-coupled device (CCD) camera. The samples for this purpose were prepared as droplet on carbon-coated copper grids and left for drying overnight in vacuum. HRTEM was investigated by JEOL-JEM 2100, Japan, operating at an accelerating voltage of 200 kV and beam current 116 mA with lanthanum hexaboride target. The gas sorption experiment was carried out using a Micromeritics 3Flex instrument. 20–25 mg of sample was taken in a 6 mm sample holder without rod. The samples were degassed at 90 ^{0}C for 2 h prior to the experiment. Ultraviolet-visible (UV-vis) absorption spectrum of samples was performed on Varian Cary 5000 UV-Visible spectrophotometer. The XPS experiments were recorded in an ultra-high vacuum (UHV) system with the surface analysis system (ESCALAB 250Xi, Thermo Fisher Scientific, Waltham, MAt) at the room temperature base pressure of the analysis chamber during the measurements was kept lower than $1.0 \times 10{-}9$ mbar. For XPS Al Ka radiation (hν = 1486.6 eV) from a monochromatized X-

ray source. Atomic force microscopy (AFM) was perfomed on a scanning probe microscope (SPM), Model Multiview-1000. Commercial Hitachi Fluorescence spectrophotometer (model no. F-7000) is used for PL measurement. EPR spectra were recorded on Bruker ELEXSYS 580.STEM-HADDF image were taken on FEG-HIGH RESOLUTION-CRYO-ANALYTICAL TEM machine.(Model number -JEM 2100F). All electrochemical work is carried on a CHI 7086E electrochemical workstation (CHI instruments Inc.). The density of state (DOS) and partial density of states (PDOS) of WS_2 and $PNEWS_2$ were calculated by using the Wien2k package with the self-consistent full potential linearized-augmented plane wave (F-LAPW) [1] method comprising of generalized gradient approximation. within Density functional theory (DFT employed to calculate the band and density of state (DOS) of sample of WS_2 and 1T-$PNEWS_2$.

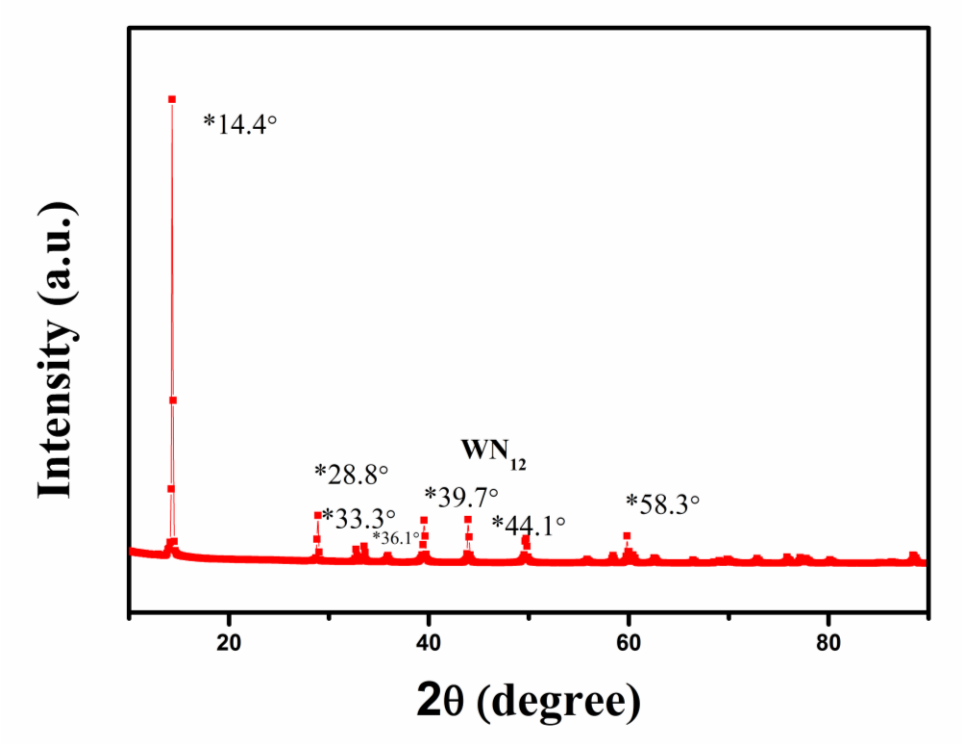

Fig. S2 XRD of WN_{12}.

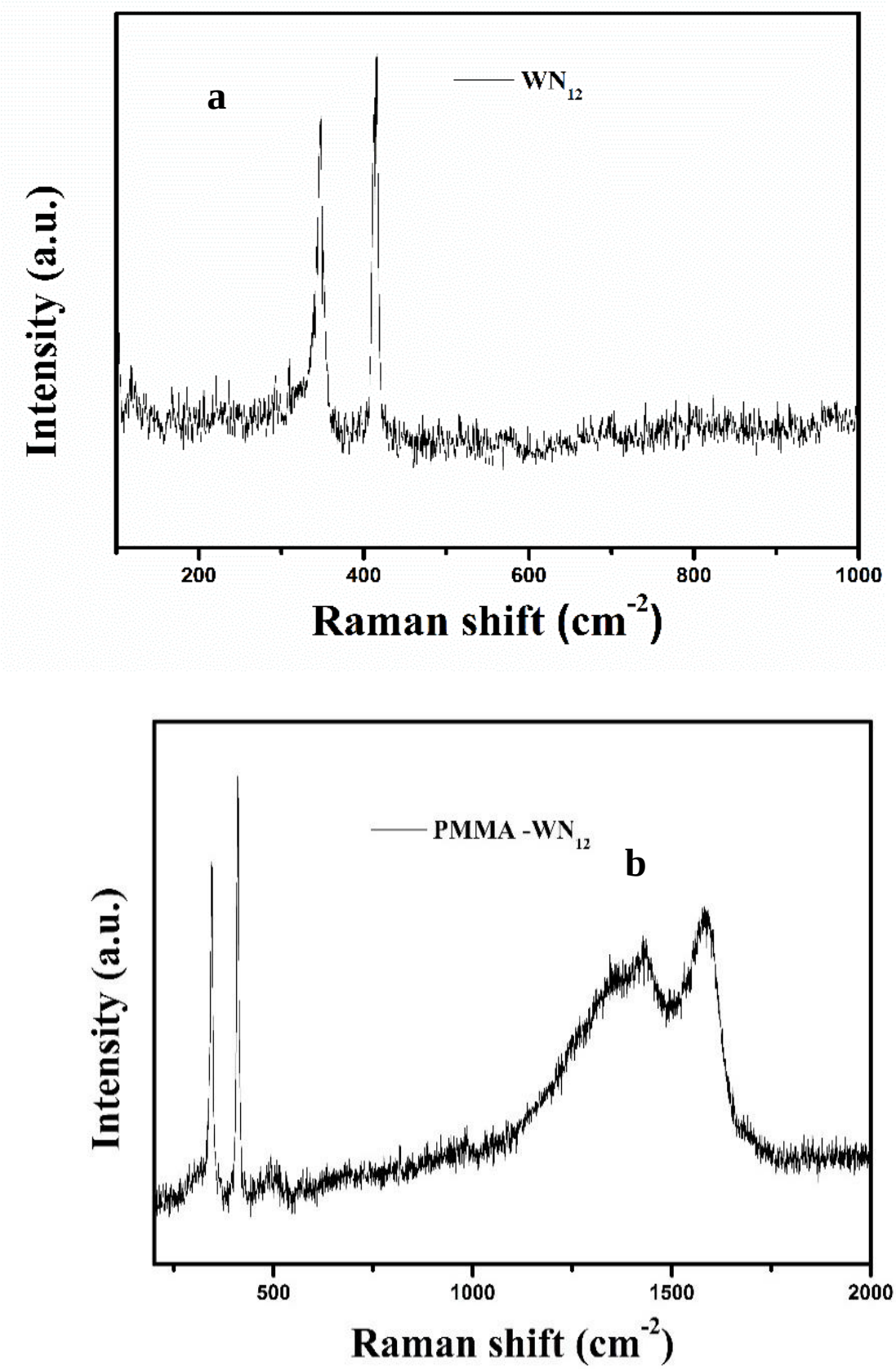

Fig. S3 Raman spectra of a) WN_{12} b) PMMA-WN_{12}.

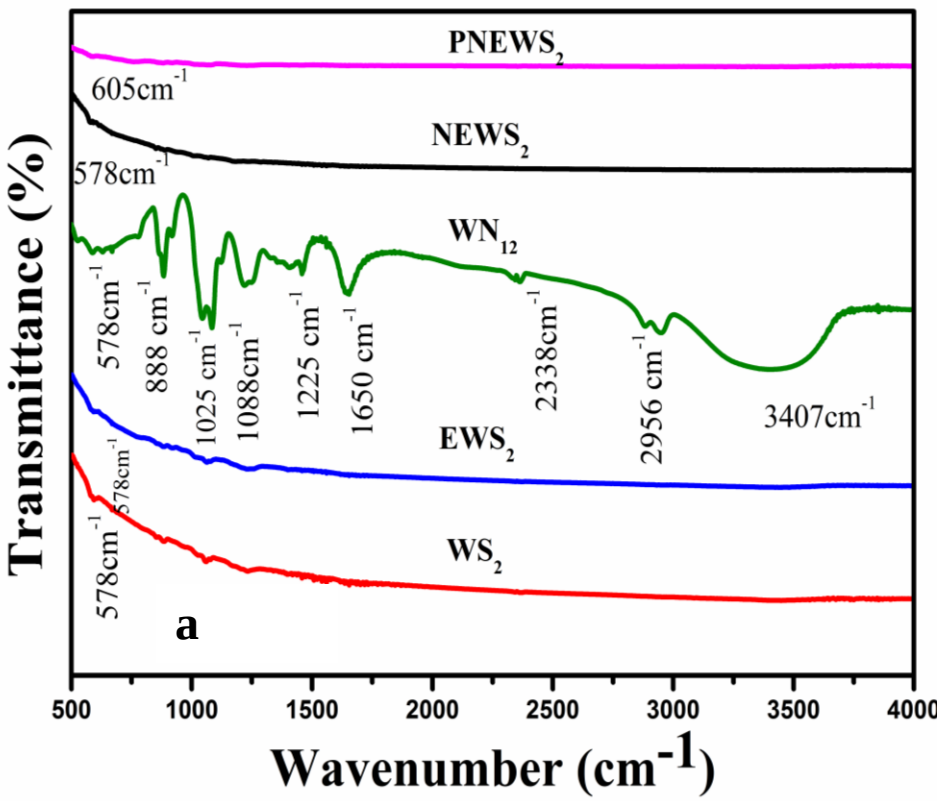

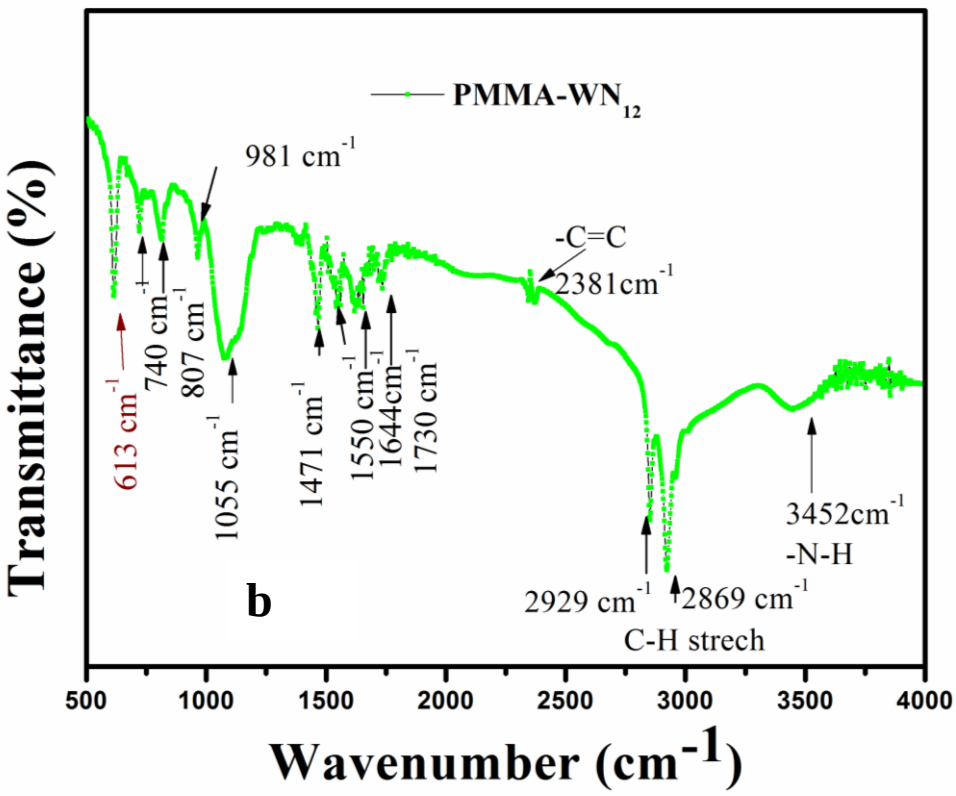

Fig. S4 IR spectra of a)WS_2, EWS_2, WN_{12}, $NEWS_2$ and $PNEWS_2$ b) PMMA-WN_{12}.

Fig. S4 shows FT-IR spectra of bulk WS_2, EWS_2, $NEWS_2$, $PNEWS_2$ in the range of 400-4000 cm^{-1}. A common peak appeared is at ~ 578 cm^{-1} corresponding to metal (W)-sulfur (S) bond in all samples.[2] WN_{12} showed appearance of peaks at ~ 3407, 2950, 1650, 1225 cm^{-1} corresponding to $–NH_2$ strech, $-CH_2$ asymetric strch, C=C strech and =C-H bending vibration respectively [3] The presence of peaks corresponding to N-H stretching (3452cm^{-1}) and alkyl C-H stretching frequency (2850 cm^{-1}) confirmed presence of oleyl amine in WN_{12}.[3] The spectra of WN_{12} film deposited on PMMA consist of peaks corresponding to =CH bending (1471 cm^{-1}), keto group (1730 cm^{-1}).[4] In contrast, these peaks disappeared in $NEWS_2$ and $PNEWS_2$ indicating successful expulsion of PMMA and oleyl amine on washing with acetone and toluene washing respectively.

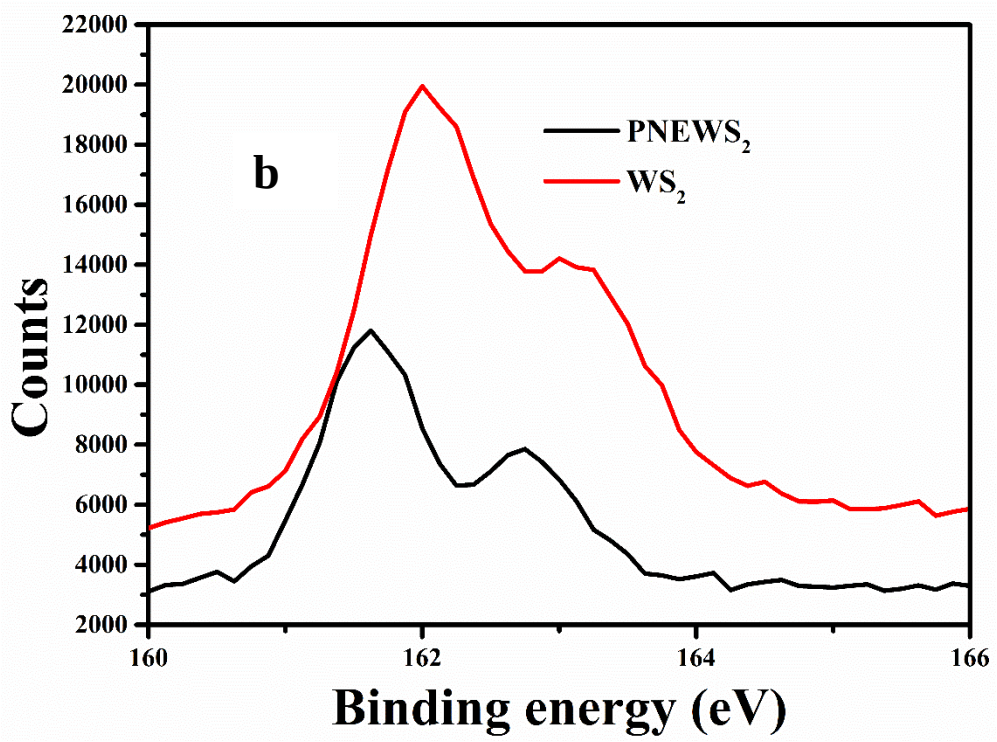

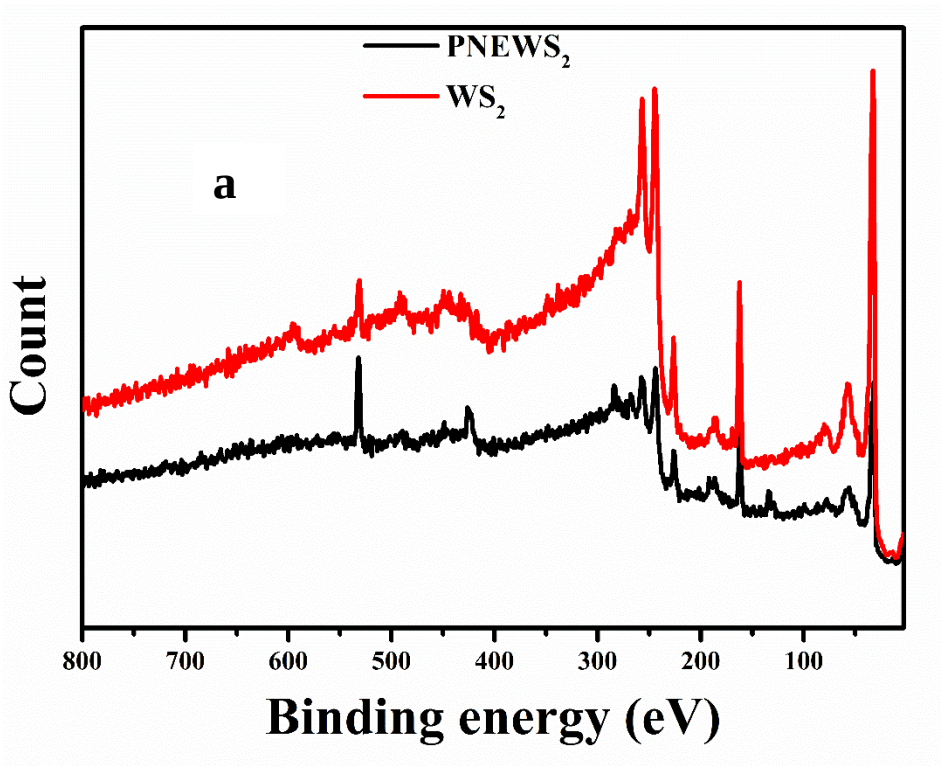

Fig. S5 (a) XPS spectrum of PNEWS$_2$ and WS$_2$. (b) S2P intensity of PNEWS$_2$ and WS$_2$.

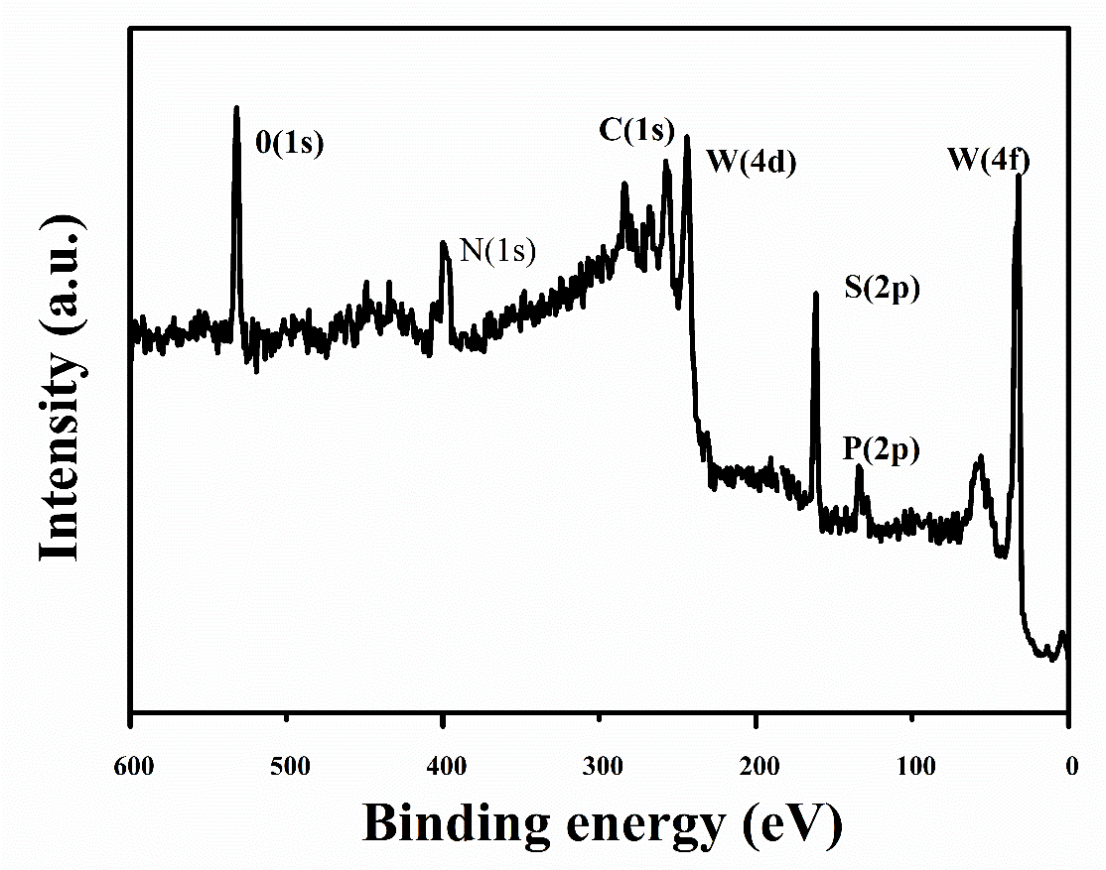

Fig. S6 XPS of $PNEWS_2$.

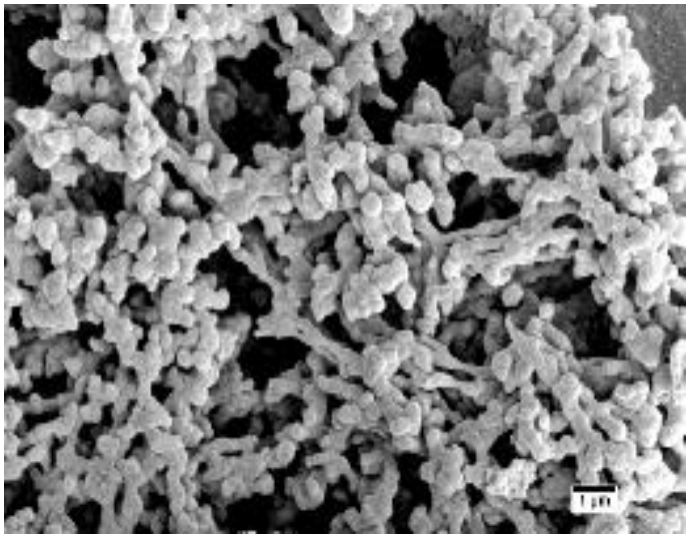

(c)

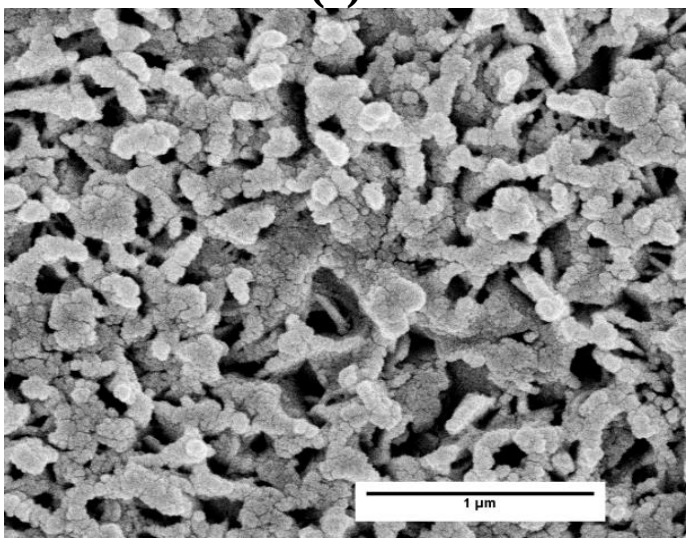

(b)

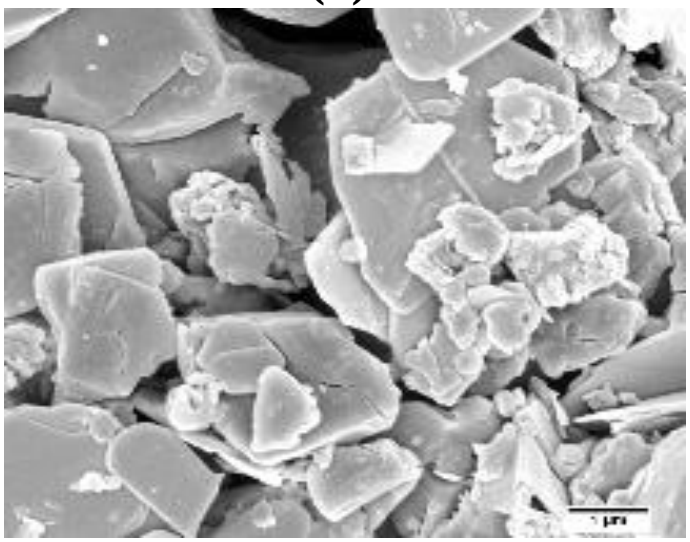

(a)

Fig. S7 a) FESEM image EWS_2, b) FESEM image of $NEWS_2$, c) FESEM image of $PNEWS_2$.

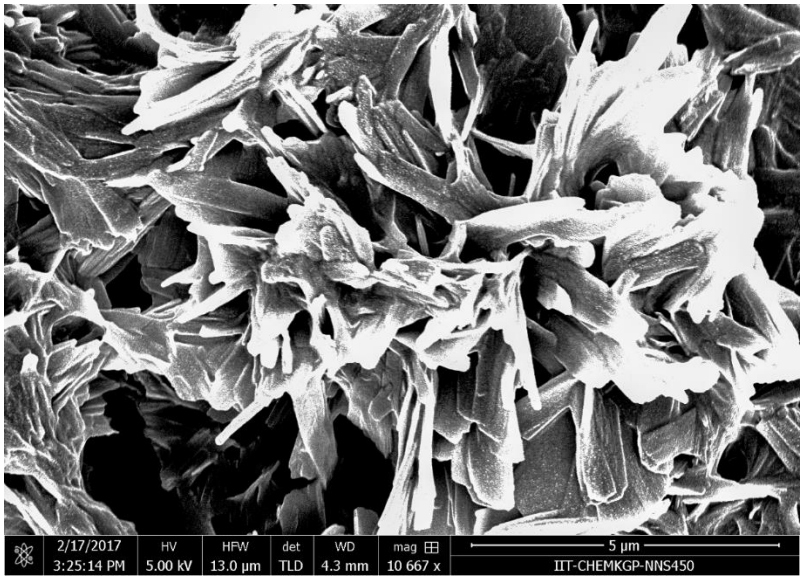

(b)

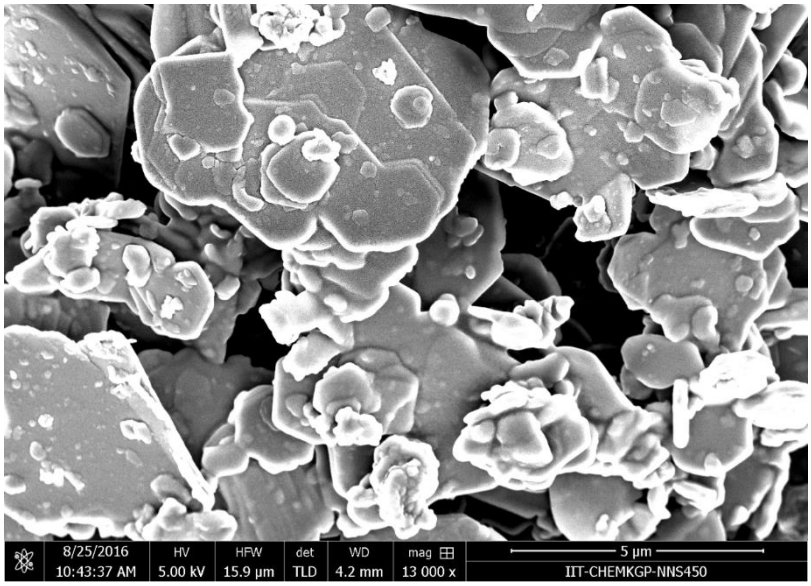

(a)

Fig. S8 FE-SEM image of a) WS_2, b) WN_{12}.

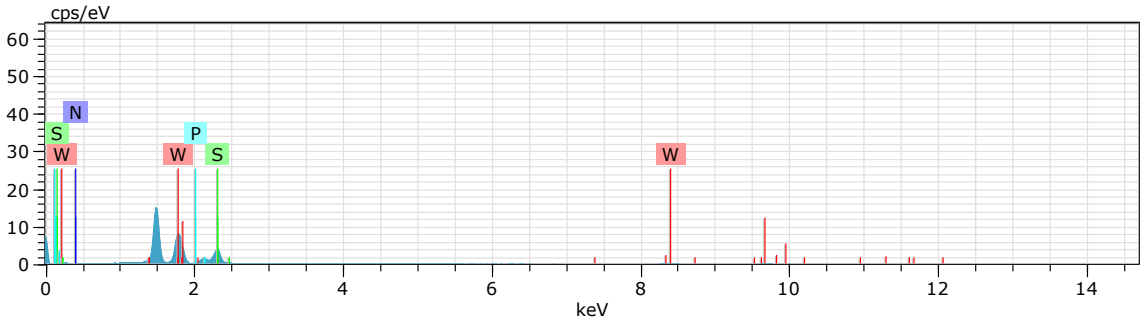

(a)

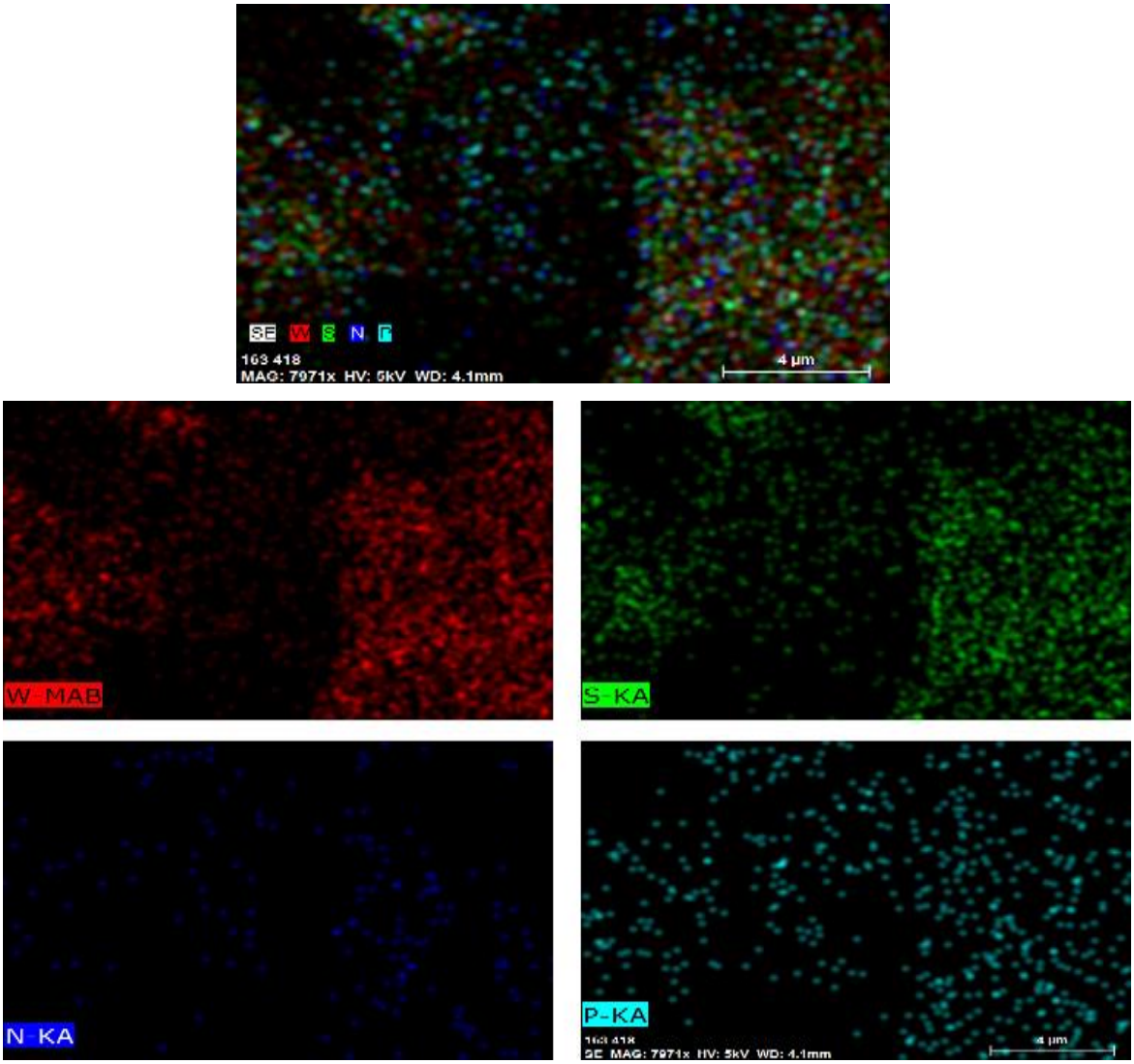

(b)

Fig. S9 a) EDS pattern of $PNEWS_2$ and b) Mapping image of $PNEWS_2$.

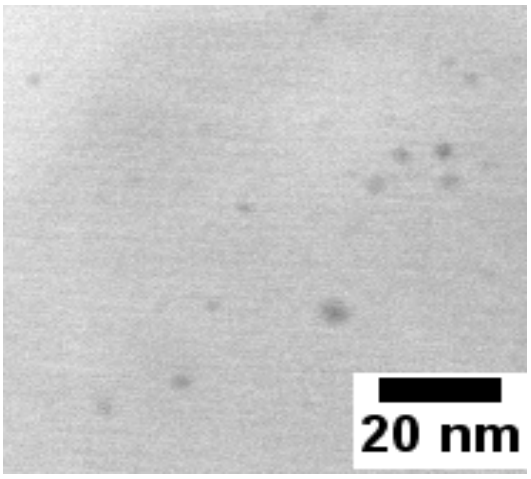

(b)

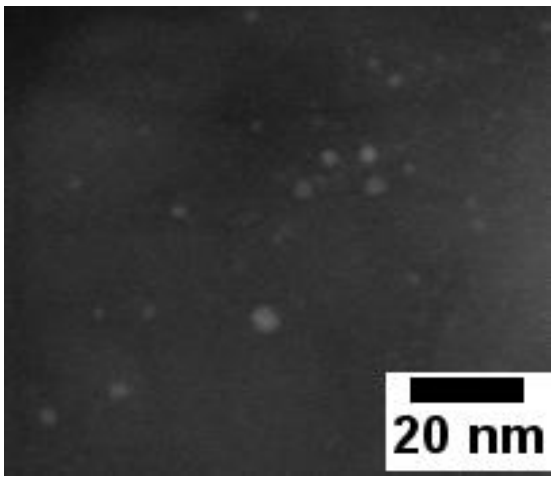

(a)

Fig. S10 HAADF –STEM (a) bright and (b) dark field image of PNEWS$_2$

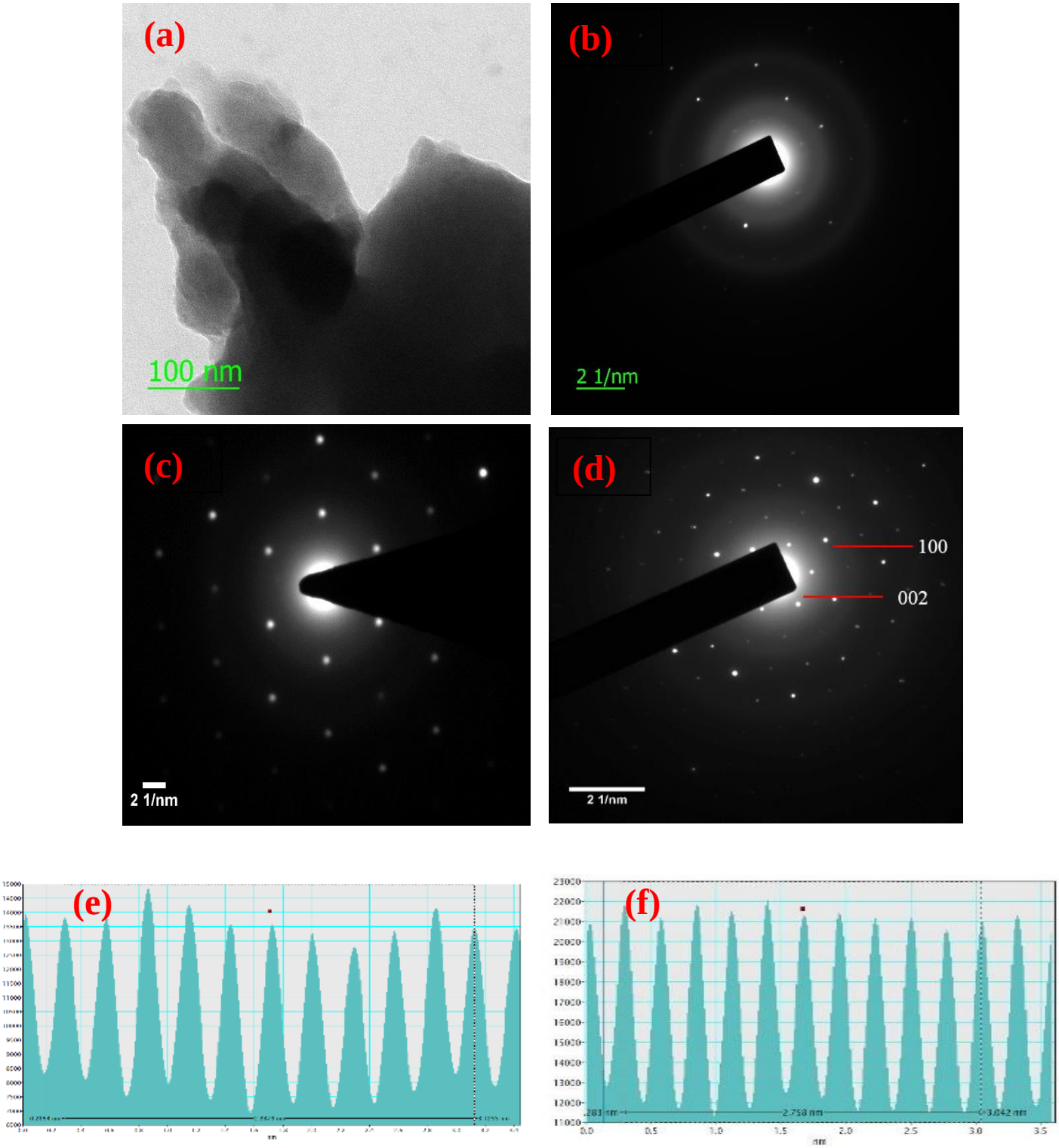

Fig. S11 a) HRTEM Image of PMMA-WN_{12}, b) SAED pattern of PMMA-WN_{12},(By HRTEM analysis), c) SAED pattern of $NEWS_2$ and d) $PNEWS_2$ by TEM analysis. (e) $NEWS_2$ shows summary of d_{100} spacing.(f) $PNEWS_2$ shows summary of d_{100} spacing).

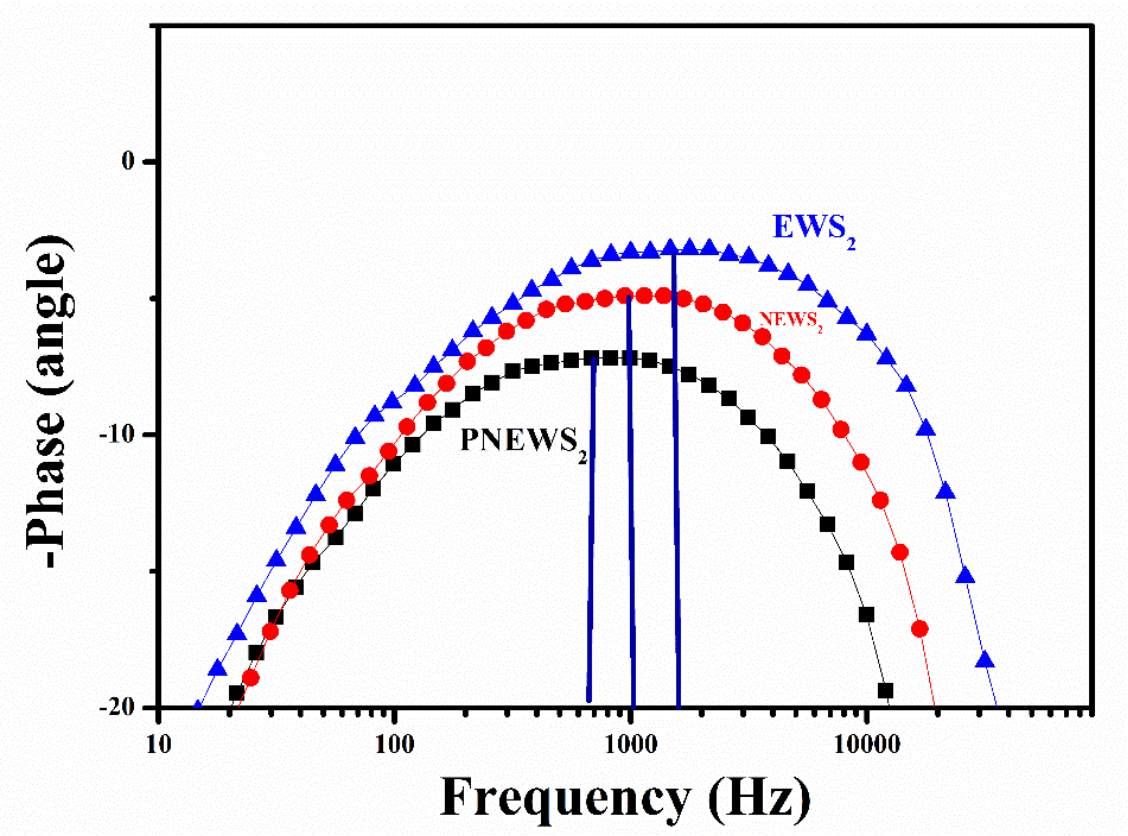

Fig. S12 Lifetime of different catalysts

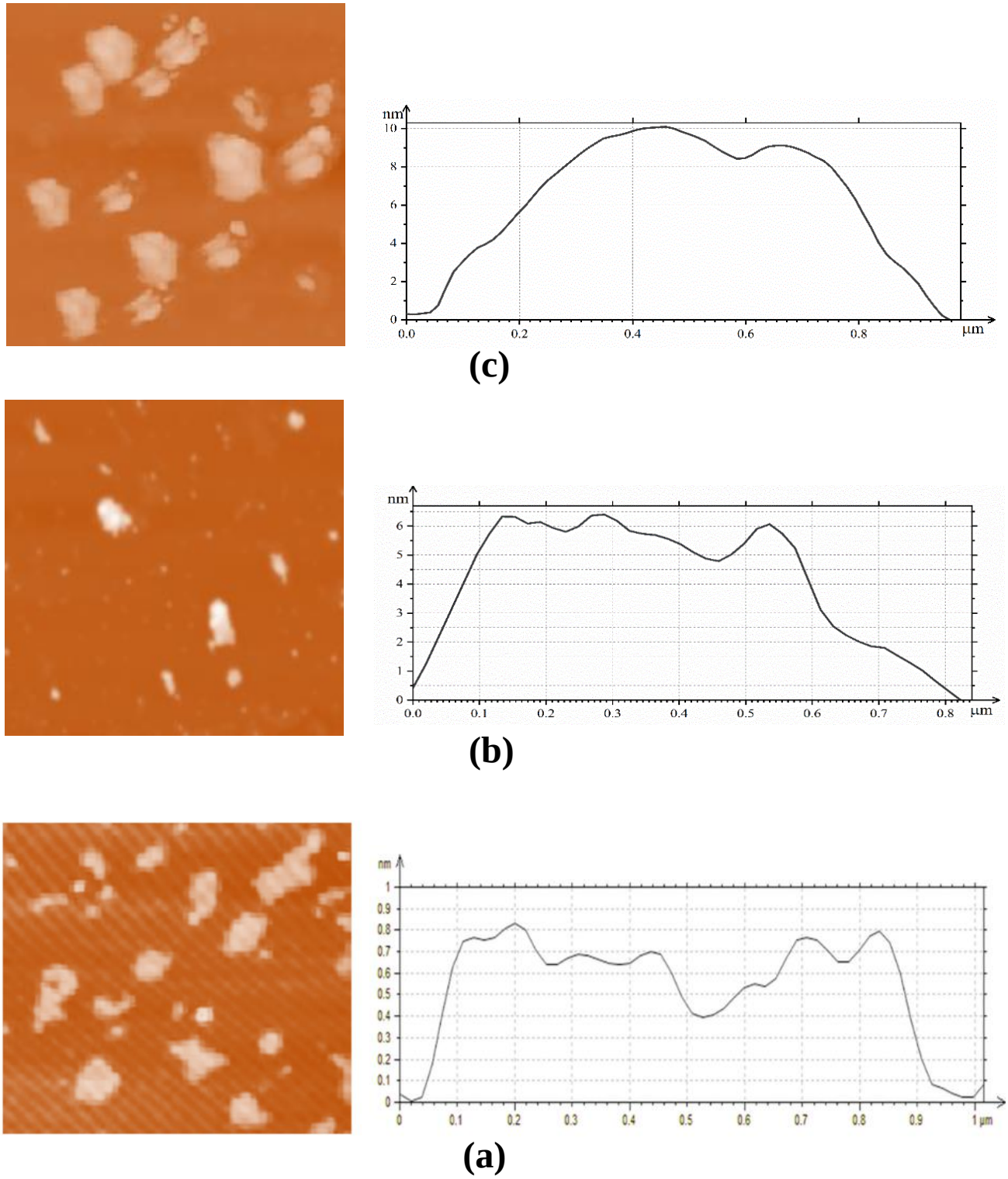

Fig. S13 AFM image and height-length profile of a) $PNEWS_2$ b) $NEWS_2$ and c) EWS_2.

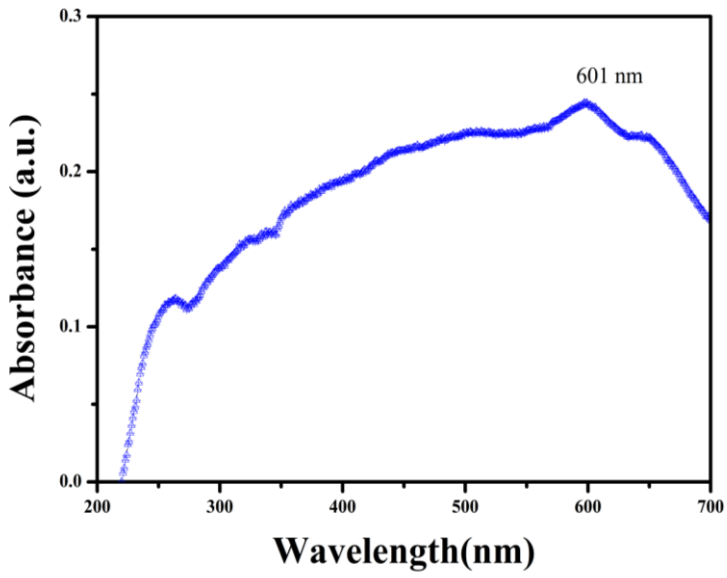

Fig. S14 UV spectrum of $PNEWS_2$.

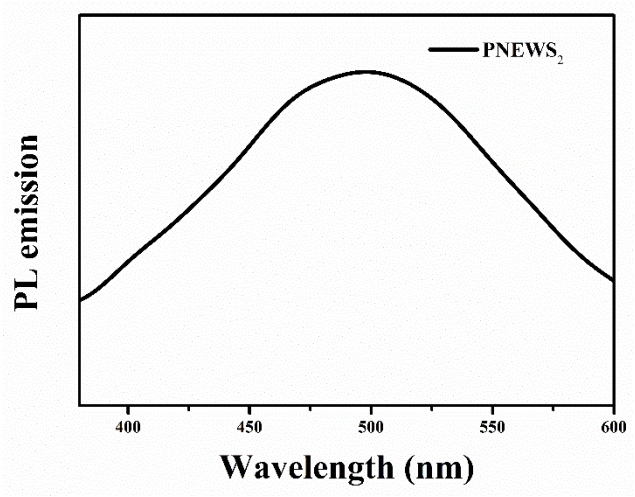

Fig. S15 PL Spectra of $PNEWS_2$.

Fig. S16 represent N_2 adsorption–desorption isotherms and pore size distribution in ingformaation of mesopore associate with micro pores. Further, it is noted that $PNEWS_2$ exhibited significantly higher specific surface area (220 m^2g^{-1}) compared to $NEWS_2$ (54.5 m^2g^{-1}) and EWS_2 (45.9 m^2g^{-1}). The enhanced surface area and pore volume of $PNEWS_2$ could be ascribed to expulsion of PH_3 gas leadfing to the the further exfoliation of $PNEWS_2$.[5]Such siognificantly higher higher specific surface area and porosity of $PNEWS_2$ is likely to provide abundant exposed edges as well as catalytic sites for HER.

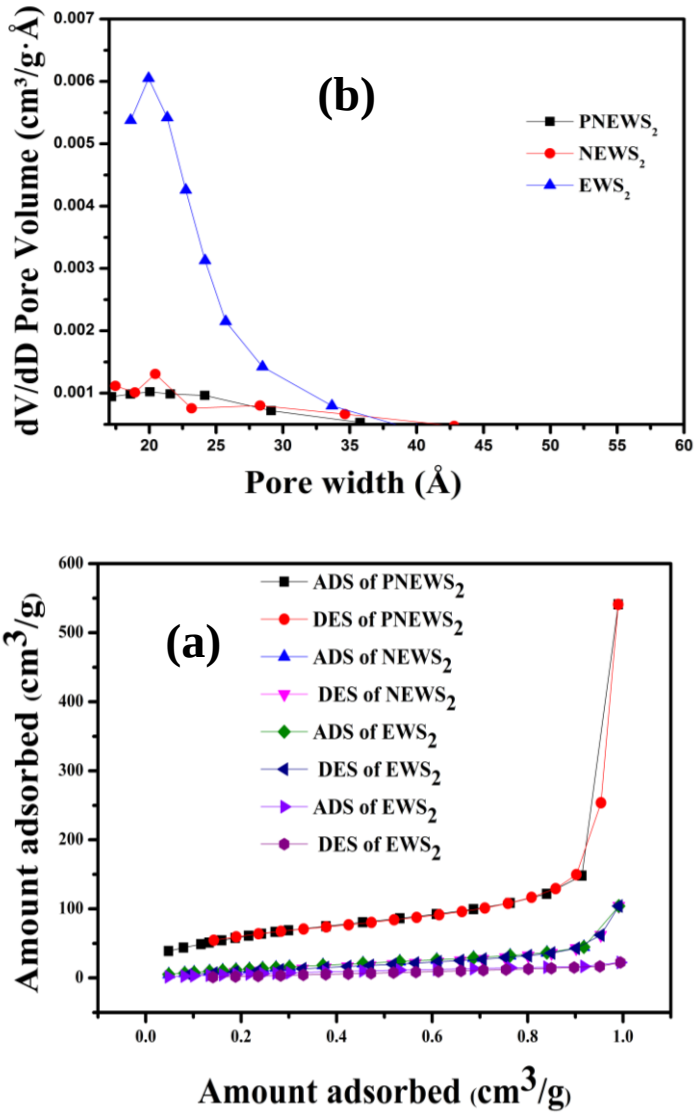

Fig. S16 a) N_2 adsorption–desorption isotherms and b) Pore size distribution in $PNEWS_2$, $NEWS_2$, EWS_2.

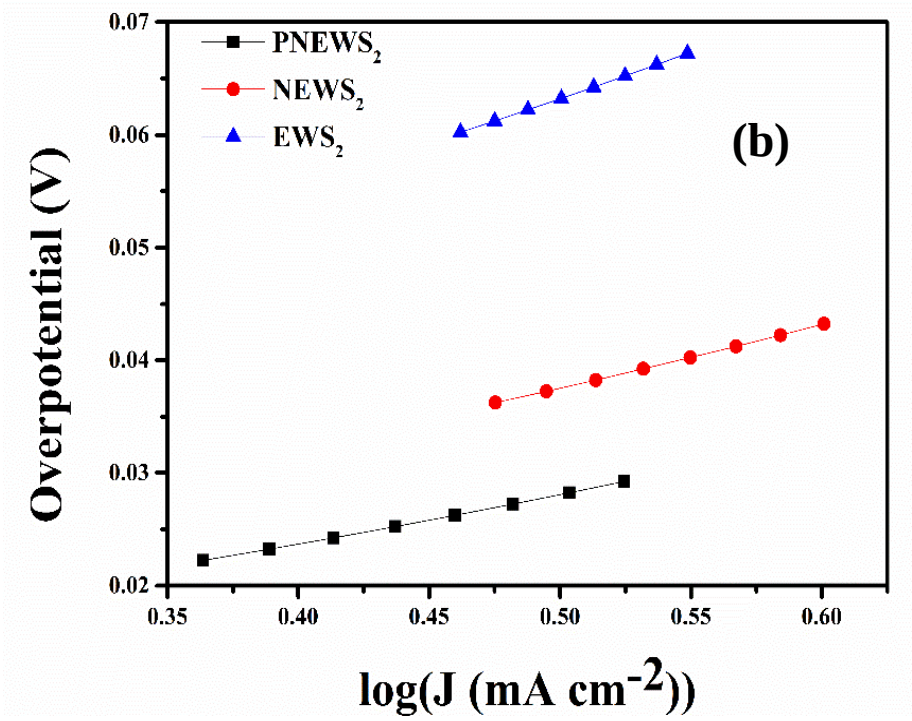

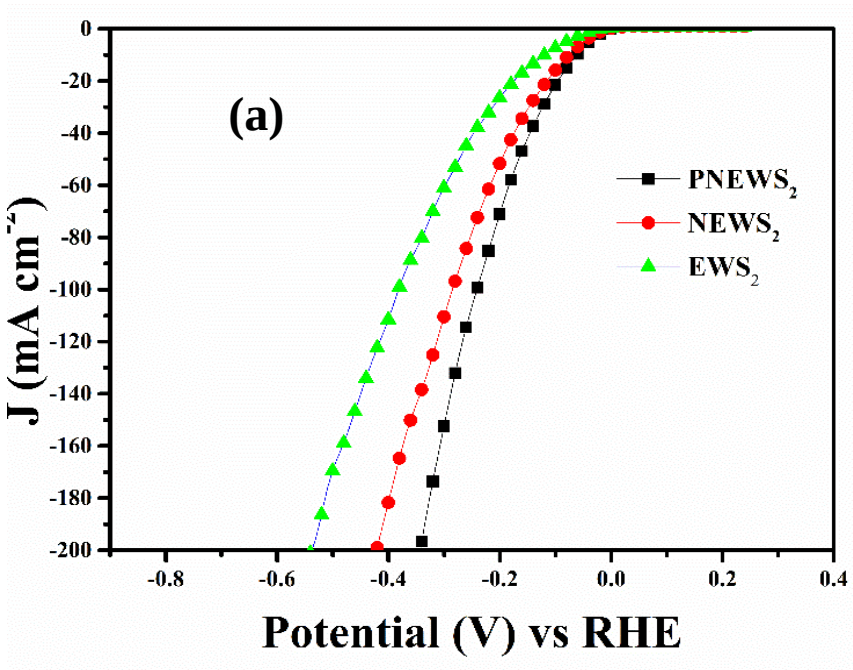

Fig. S17 a) LSV of catalysts EWS_2, $NEWS_2$ and $PNEWS_2$ at 1mV/ sec and its b) corresponding Tafel slope in 0.5molar H_2SO_4.

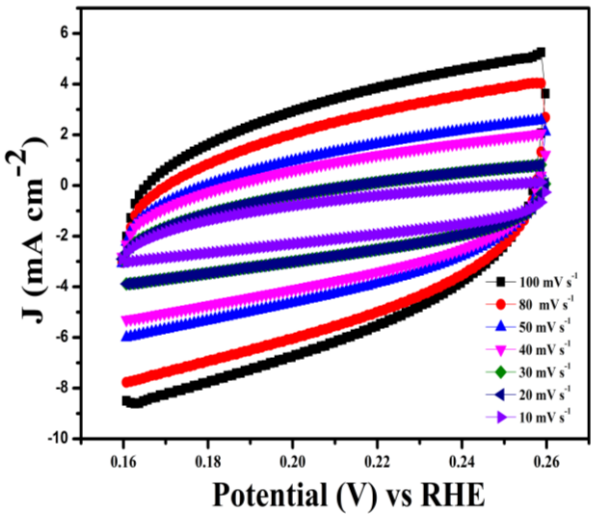

Fig. S18 Cyclic voltammograms of PNEWS$_2$ measured at different scan rate.

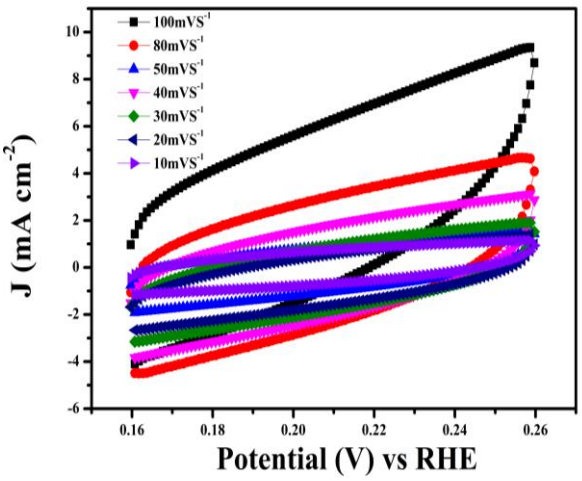

Fig. S19 Cyclic voltammograms of NEWS$_2$, measured at different scan rate.

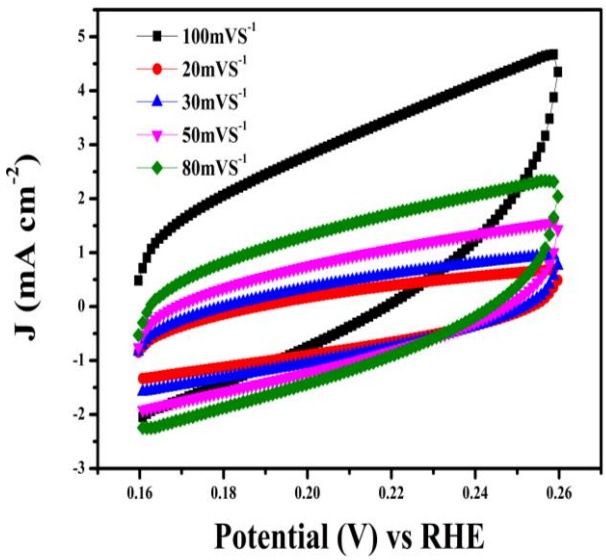

Fig.S20 Cyclic voltammograms of EWS$_2$, measured at different scan rate.

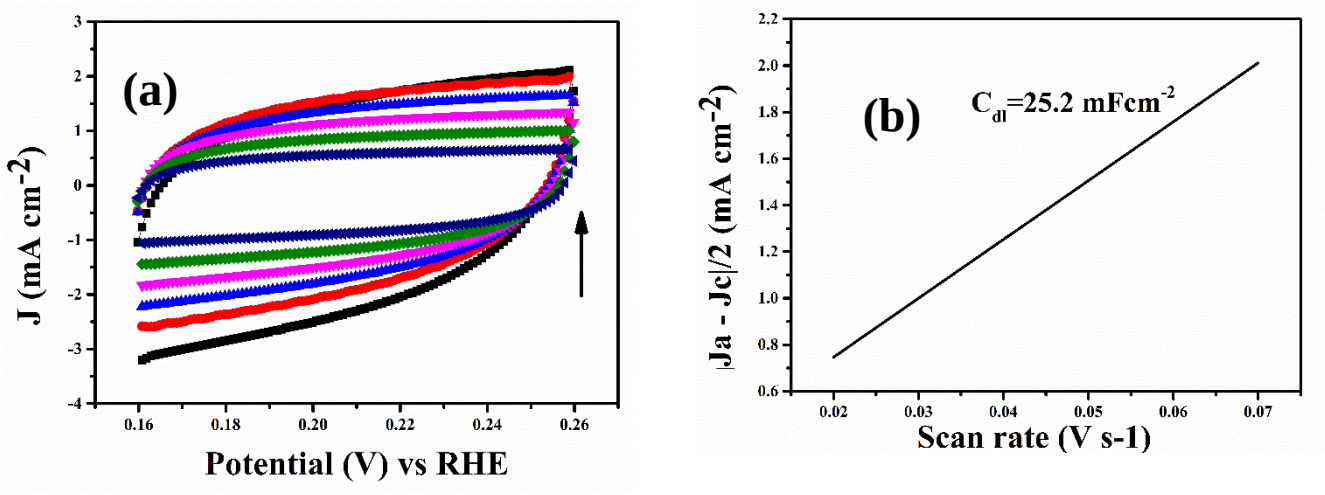

Fig.S21 (a) CV of Pt/C (10 wt%) at (20-80) mVs^{-1} scan rate and its (b) corresponding double layer capacitance.

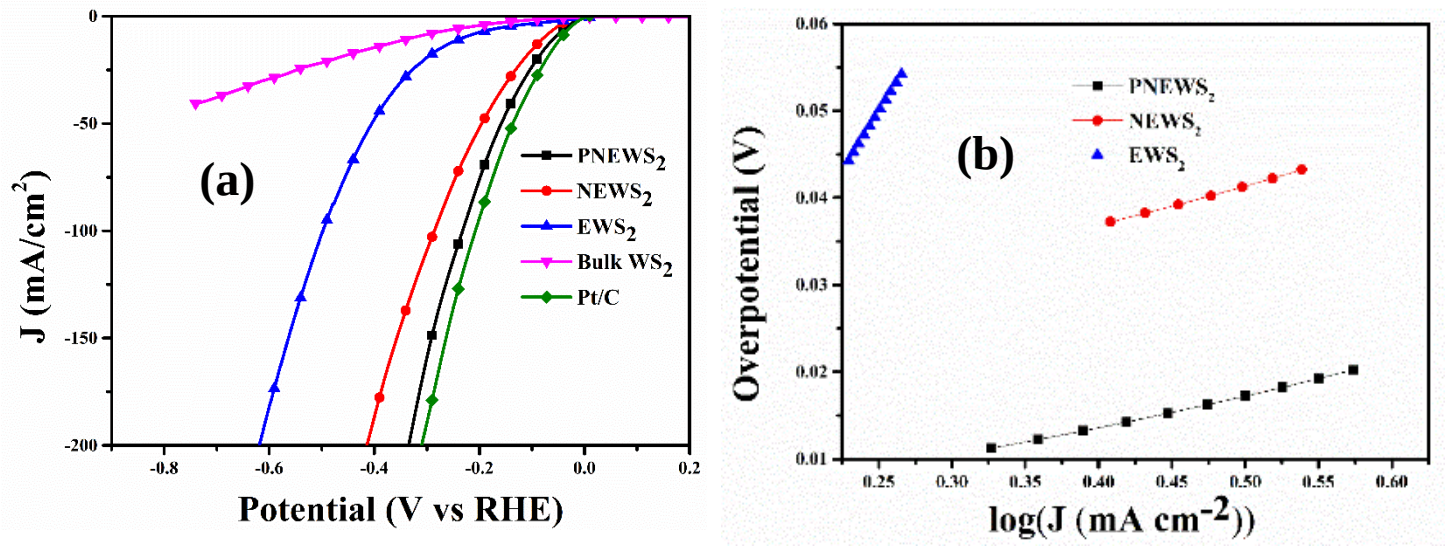

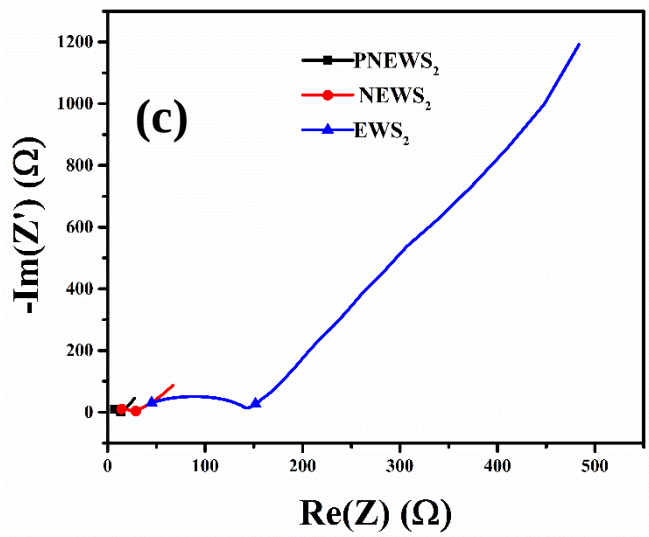

Fig. S22 Accounting graphite as counter electrode **(**a) Total current density (J) vs Potential curve of catalyst in 0.5 M H_2SO_4.(b) Tafel slope of catalysts in 0.5 Molar H_2S0_4. (c) Nyquist plot of catalysts.

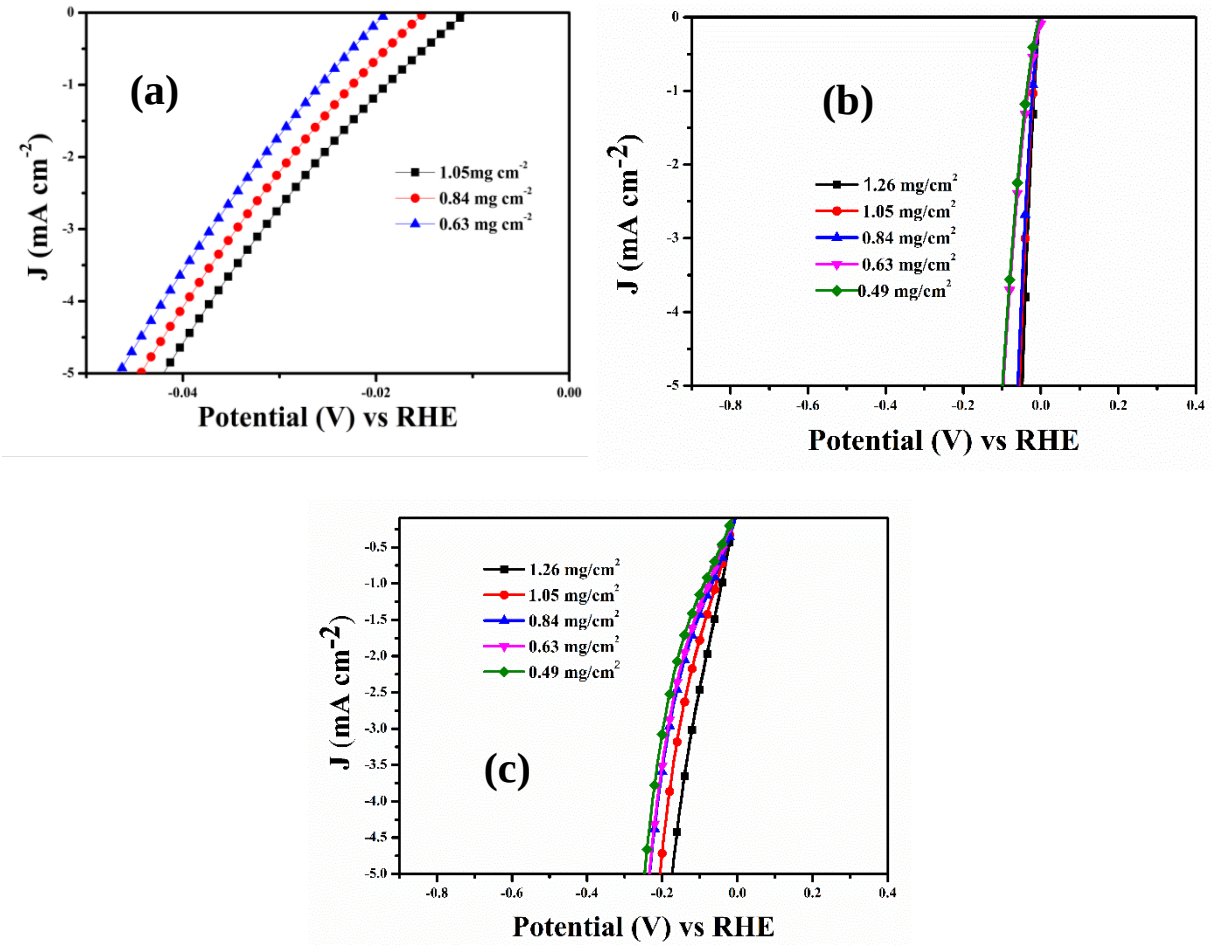

Fig. S23 Variation of current density versus potential of at different catalyst loadings. a) $PNEWS_2$ b) $NEWS_2$ c) EWS_2.

Fig. S23 show **v**ariation of current density versus potential of $PNEWS_2$ at different catalyst loadings. It is noted that current density increase linearly with mass loadings of $PNEWS_2$. This clearly suggest that increased roughness factor (RF) could account for enhanced HER due to the presence of more number active sites accessible to perform the catalysis.[6, 7]

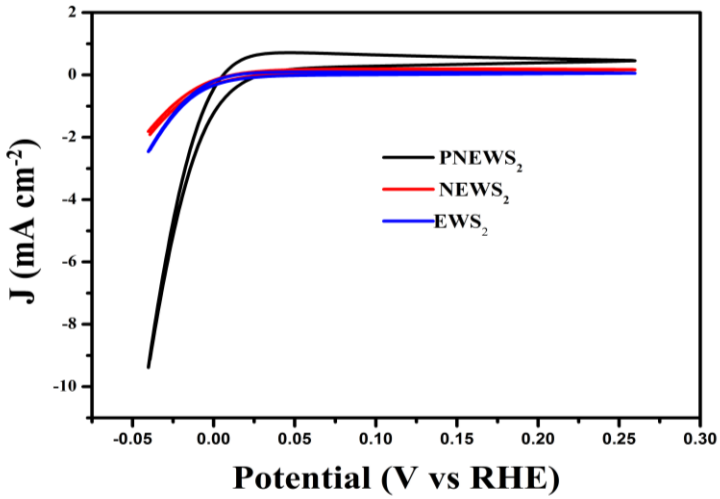

Fig. S24 Cyclic voltammograms of EWS_2, $NEWS_2$ and $PNEWS_2$ (Scan rate: 50 mV s^{-1}).

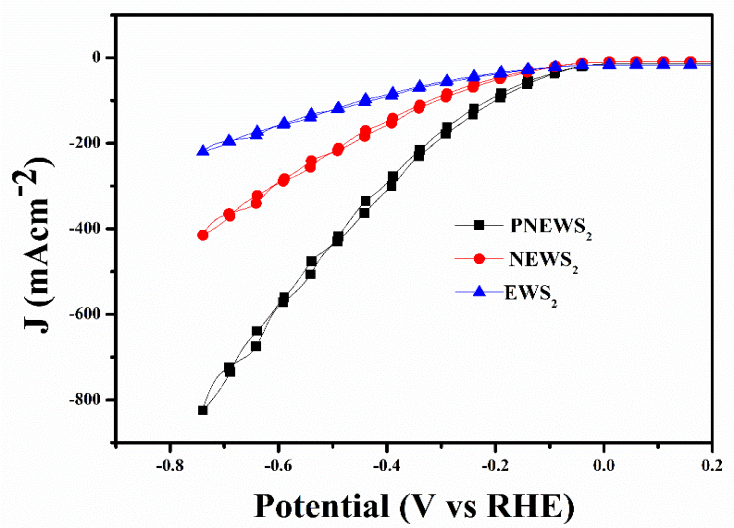

Fig. S25 CV of EWS_2,$NEWS_2$ and $PNEWS_2$ after 1000 cycle

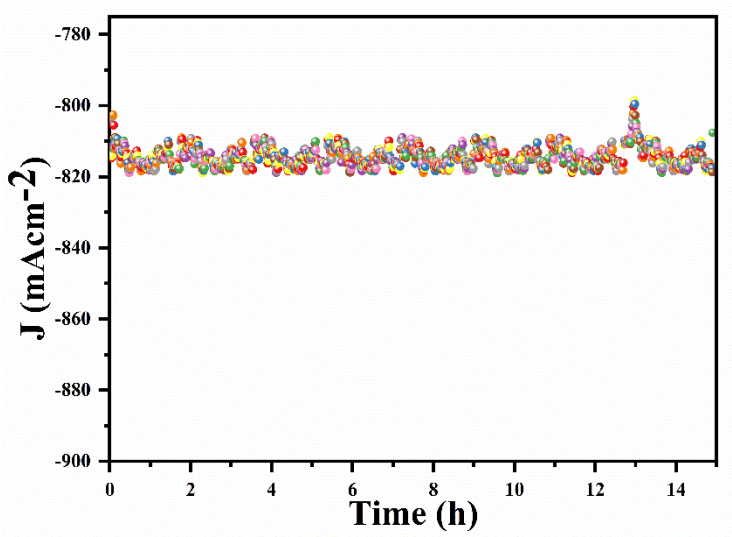

Fig. S26 $PNEWS_2$ shows 15 hour i-t test at - 0.74 V.

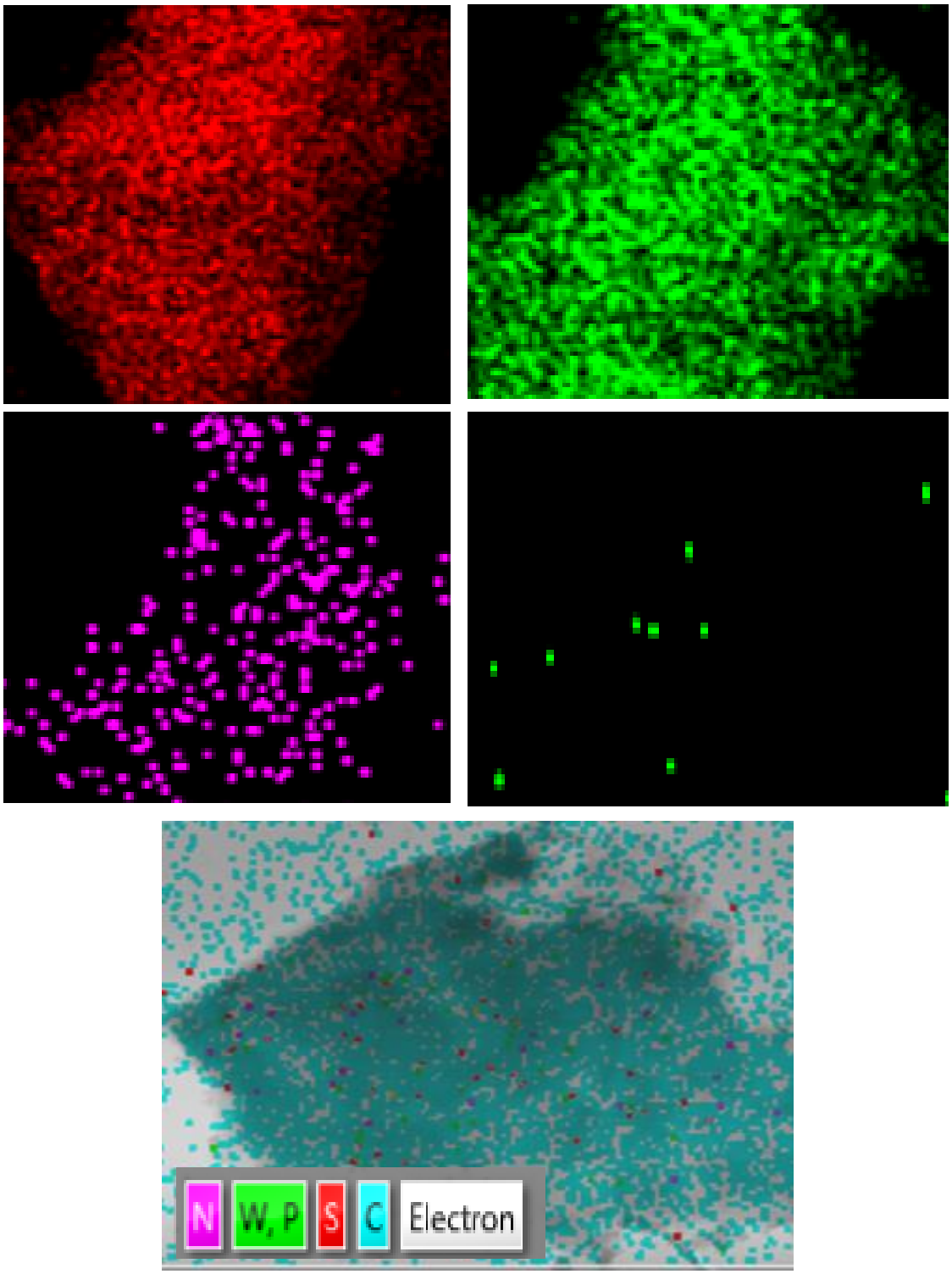

Fig. S27 Elemental mapping image of catalyst $PNEWS_2$ after 15 hour electroctalysis.

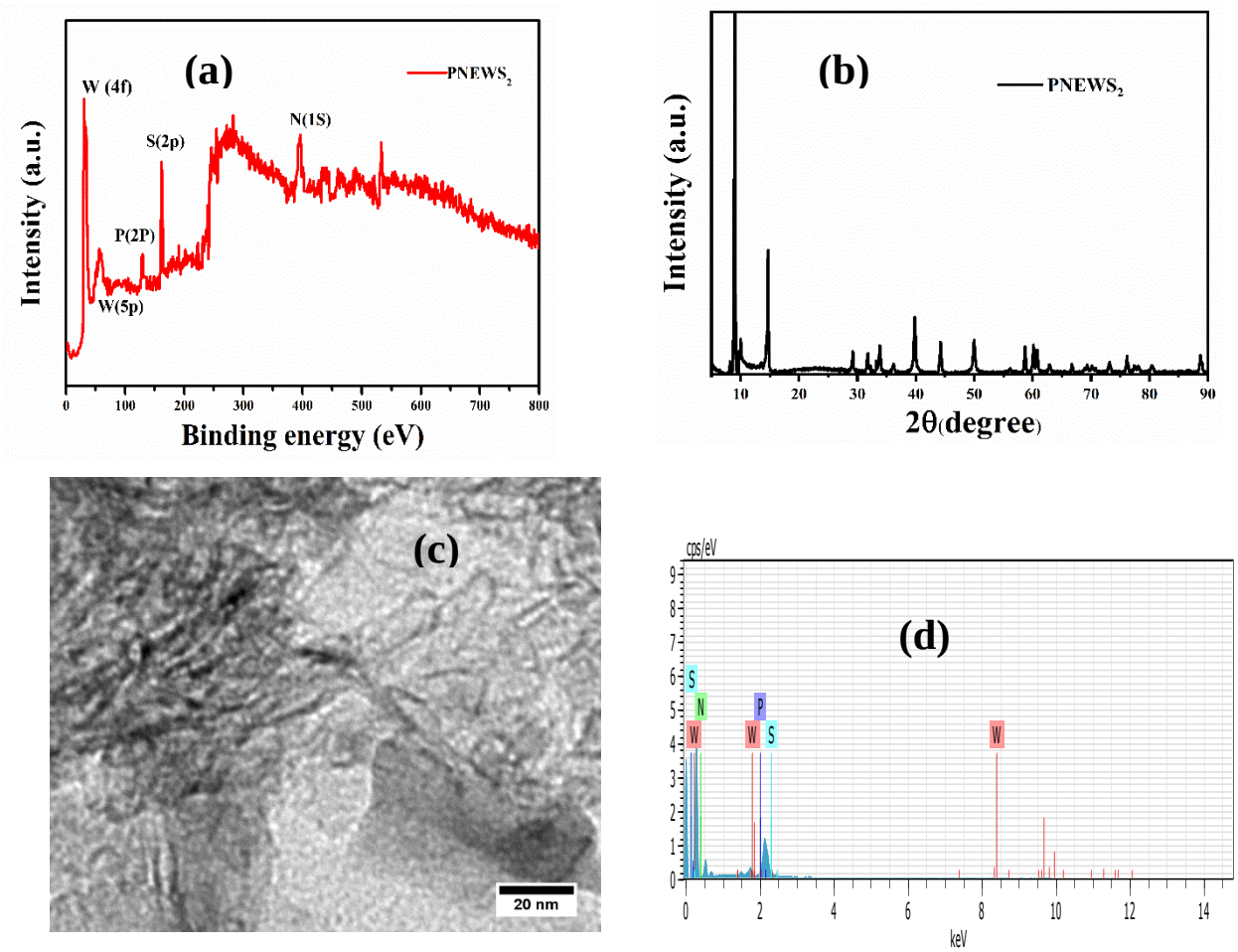

Fig. S28 After 15 hour electrocatalysis of catalyst $PNEWS_2$ a) XPS b) XRD c) TEM d) EDS

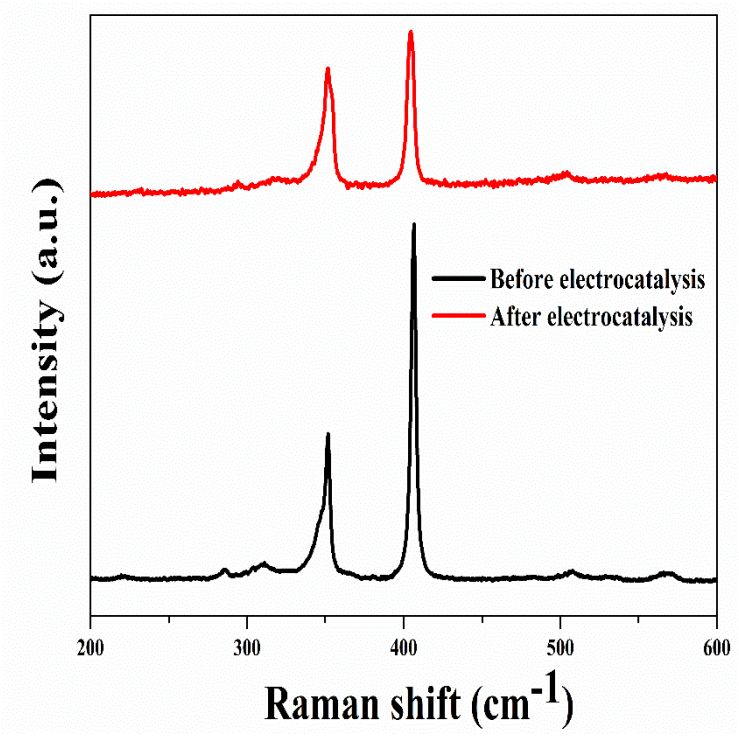

Fig. S29 Raman spectra after 10 hour electrocatalysis of catalyst $PNEWS_2$.

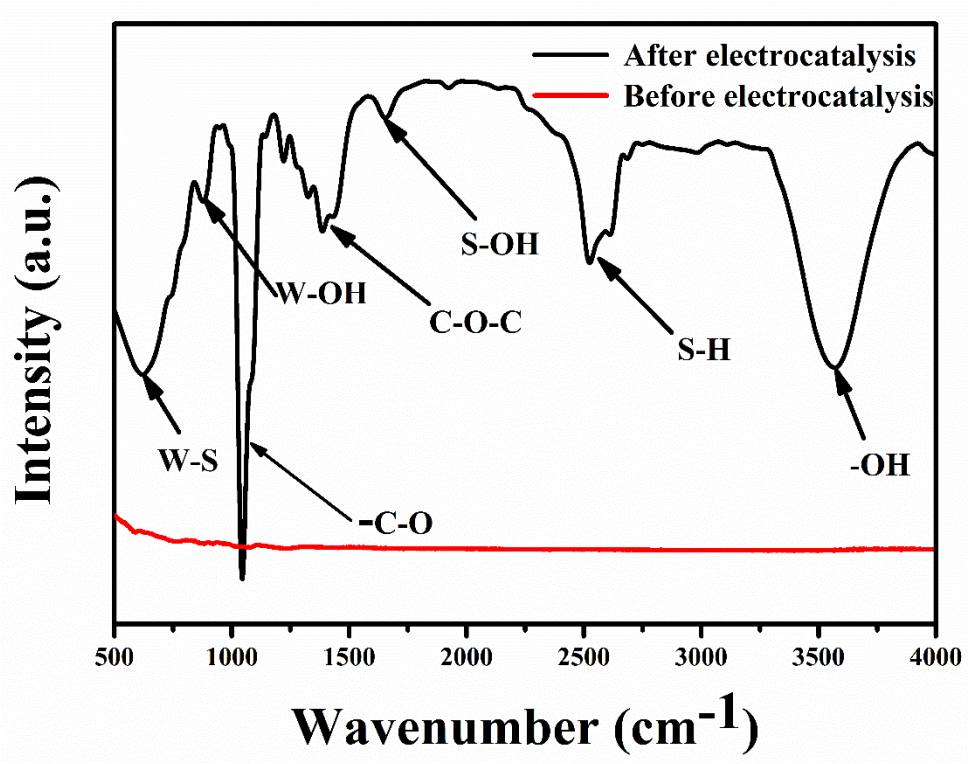

Fig. S30 IR spectra of catalyst $PNEWS_2$ before and after electrocatalysis.

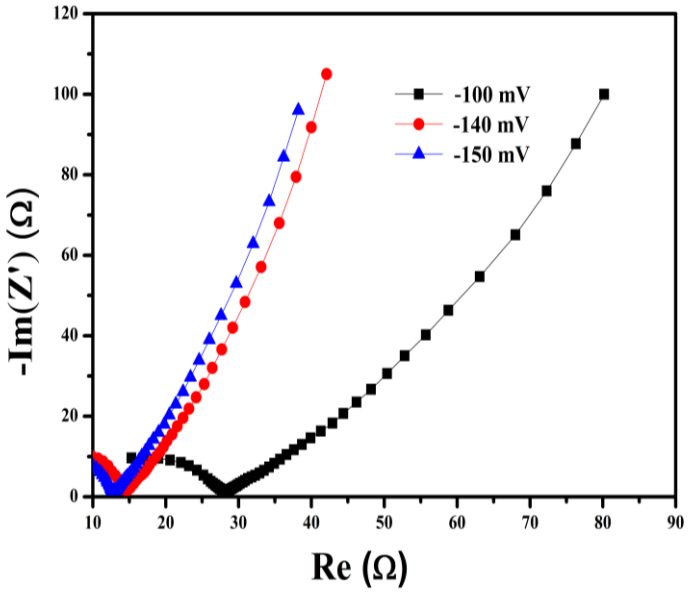

Fig. S31 Impedence spectra of $PNEWS_2$ at -100, -140 and -150 mV potential.

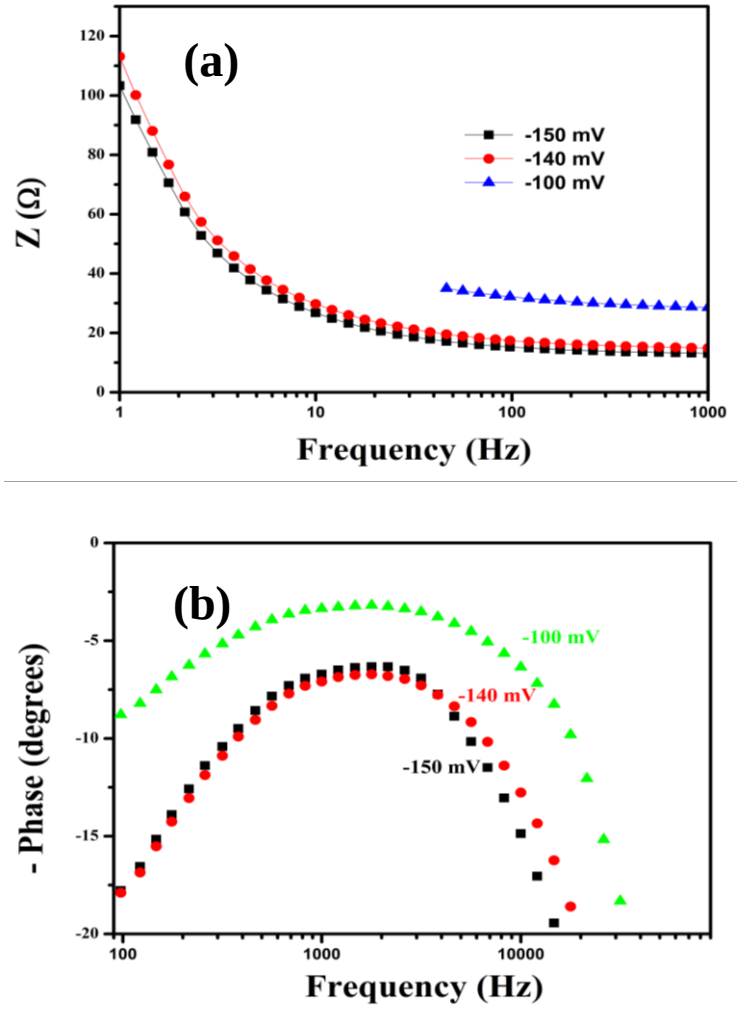

Fig. S32. a) Impedance versus frequency plots and b) Phase versus frequency plots of $PNEWS_2$ at -100, -140 and -150 mV.

Table S1. Comparative performance of different electrocatalysts on HER.

Catalysts	Onset-potential (mV)	Tafel slope (mV dec^{-1})	Current density ($mAcm^{-2}$)	Overpotential (mV)	Ref.
WS_2@heteroatom dopedgraphene film	-	52.7	10	125	8
C_3N_4@NG	-	51.5	10	240	9
MoS_2 nanoparticles	90	69	-	-	10
MoS_2 nanoplates	90	53			11
MoS_2 formed on mesoporousgraphene	-	85	10	200	12
Co−CoO/N-doped carbon hybrids	85	115	10	235	13
WS_2/rGO		73	10	229	14
CoP/rGO	13	50	10	105	15
$WS_{2(1-x)}P_{2x}$	-	71	10	98	16
er-WS_2-Pt	-	27	10	30	17
Exfoliated WS_2 Nanodots	90	51	-	-	18
3D WS_2 Nanolayers@Heteroatom-Doped Graphene Films	-	52.7	10	125	19
PNEWS$_2$	**11**	**35**	**10**	**59**	**This work**

Table S2. Summary of HER performance with catalyst loading.

Catalyst	Catalyst loading	Current density (mA/cm^2)	Overpotential (mV)	Tafel slope (mV $decade^{-1}$)	Ref.
Exfoliated WS_2	0.1-0.2 μg cm^{-2}	10	80-100	60	20
CoMoSx	50 μg cm^{-2}	5	207	-	21
$WO_{2.9}$	0.285 mg cm^{-2}	10	70	50	22
Edge terminated MoS_2	0.28 mg cm^{-2}	10	150	49	23
Pt-MoS_2	75 μg cm^{-2}	10	53	40	24
Co-NG	0.285 mg cm^{-2}	0.3	30	82	25
MoP_2 nanosheet	7.80 mg cm^{-2}	10	58	34.6	26
P-W_2C@N	3.50 mg cm^{-2}	10	89	53	27
$NiCo_2Px$ Nanowires	5.90 mg cm^{-2}	10	104	59.6	28
PNEWS_2	**1.4 mg cm^{-2}**	**10**	**59**	**35**	**This work**

Reference

1. S. O. Kumar, V. Shukla and S. K. Srivastava, *Mater. Let*,. 2018, **225**, 134-137.
2. H. Dong, D. Chen, K. Wang and R. Zhang, *Nanoscale Res.Lett.*, 2016, **11**, 409 (1-14).
3. D. Thangaraju, R. Karthikeyan, N. Prakash, S. M. Babu and Y. Hayakawa, *Dalton Trans.*, 2015, **44**, 15031-15041.
4. Y. Liu, W. Hu, Z. Lu and C. M. Li, *Med. Chem.Comm.*, 2010, **1**, 132-135.
5. Y. Jin, X. Yue, C. Shu, S. Huang and P. K. Shen, *J. Mat.Chem. A.*, 2017, **5**, 2508-2513.
6. R. Kötz and M. Carlen, *Electrochim. Acta.*, 2000, **45**, 2483-2498.

7. J. D. Benck, Z. Chen, L. Y. Kuritzky, A. J. Forman and T. F. Jaramillo, *ACS Catal.*, 2012, **2**, 1916-1923.

8 J. Duan, S. Chen, B. A. Chambers, G. G. Andersson and S. Z. Qiao, *Adv.Mater.*, 2015, **27**, 4234-4241.

9. Y. Zheng, Y. Jiao, Y. Zhu, L. H. Li, Y. Han, Y. Chen, A. Du, M. Jaroniec and S. Z. Qiao, *Nat. Commun.*, 2014, **5**, 3783 (1-8).

10. T. Wang, L. Liu, Z. Zhu, P. Papakonstantinou, J. Hu, H. Liu and M. Li, *Energy Environ. Sci.*, 2013, **6**, 625-633.

11. Y. Yan, B. Xia, X. Ge, Z. Liu, J.-Y. Wang and X. Wang, *ACS Appl. Mater. Interfaces*, 2013, **5**, 12794-12798.

12. L. Liao, J. Zhu, X. Bian, L. Zhu, M. D. Scanlon, H. H. Girault and B. Liu, *Adv. Funct. Mater.*, 2013, **23**, 5326-5333.

13. H. Jin, J. Wang, D. Su, Z. Wei, Z. Pang and Y. Wang, *J. Am. Chem. Soc.*, 2015, **137**, 2688-2694.

14. T. A. Shifa, F. Wang, Z. Cheng, X. Zhan, Z. Wang, K. Liu, M. Safdar, L. Sun and J. He, *Nanoscale*, 2015, **7**, 14760-14765.

15. L. Jiao, Y.-X. Zhou and H.-L. Jiang, *Chem.Sci.*, 2016, **7**, 1690-1695.

16. T. A. Shifa, F. Wang, K. Liu, Z. Cheng, K. Xu, Z. Wang, X. Zhan, C. Jiang and J. He, *Small*, 2017, **13**, 1603706 (1-6).

17. K. Tang, X.Wang, Q.Li, C.Yan, *Adv. Mater.*, 2018, **30**, 1704779 (1-7).

18. X. Zhao, X. Ma, J. Sun, D. Li and X. Yang, *ACS Nano*, 2016, **10**, 2159-2166.

19. J.Duan, S.Chen,B.A. Chambers, G.G. Andersson, S.Z. Qiao, *Adv. Mater.* 2015, **27**, 4234-4241.

20. D. Voiry, H. Yamaguchi, J. Li, R. Silva, D. C. Alves, T. Fujita, M. Chen, T. Asefa, V. B. Shenoy and G. Eda, *Nat. Mater.*, 2013, **12**, 850-855.

21. J. Staszak-Jirkovský, C. D. Malliakas, P. P. Lopes, N. Danilovic, S. S. Kota, K.-C. Chang, B. Genorio, D. Strmcnik, V. R. Stamenkovic and M. G. Kanatzidis, *Nat. Mater.*, 2016, **15**, 197-203.

22. Y. H. Li, P. F. Liu, L. F. Pan, H. F. Wang, Z. Z. Yang, L. R. Zheng, P. Hu, H. J. Zhao, L. Gu and H. G. Yang, *Nat. Commun.*, 2015, **6**, 8064(1-7).

23. M.-R. Gao, M. K. Chan and Y. Sun, *Nat.Commun.*, 2015, **6**, 7493 (1-8).

24. X. Huang, Z. Zeng, S. Bao, M. Wang, X. Qi, Z. Fan and H. Zhang, *Nat. Commun.*, 2013, **4**, 1444 (1-8).

25. H. Fei, J. Dong, M. J. Arellano-Jiménez, G. Ye, N. D. Kim, E. L. Samuel, Z. Peng, Z. Zhu, F. Qin and J. Bao, *Nat. Commun.*, 2015, **6**, 8668 (1-8).

26. W. Zhu, C. Tang, D. Liu, J. Wang, A. M. Asiri and X. Sun, *J. Mater.Chem. A*, 2016, **4**, 7169-7173.

27. G. Yan, C. Wu, H. Tan, X. Feng, L. Yan, H. Zang and Y. Li, *J. Mater. Chem. A*, 2017, **5**, 765-772.

28. R. Zhang, X. Wang, S. Yu, T. Wen, X. Zhu, F. Yang, X. Sun, X. Wang and W. Hu, *Adv. Mater.*, 2017, **29**, 1605502 (1-6).